

AN EFFICIENT ITERATIVE THRESHOLDING METHOD FOR IMAGE SEGMENTATION *

DONG WANG [†], HAOHAN LI [‡], XIAOYU WEI [§], AND XIAOPING WANG [¶]

Abstract. We proposed an efficient iterative thresholding method for multi-phase image segmentation. The algorithm is based on minimizing piecewise constant Mumford-Shah functional in which the contour length (or perimeter) is approximated by a non-local multi-phase energy. The minimization problem is solved by an iterative method. Each iteration consists of computing simple convolutions followed by a thresholding step. The algorithm is easy to implement and has the optimal complexity $O(N \log N)$ per iteration. We also show that the iterative algorithm has the total energy decaying property. We present some numerical results to show the efficiency of our method.

Key words. Iterative thresholding, Image segmentation, Piecewise constant Mumford-Shah functional, Convolution, Fast Fourier transform

AMS subject classifications. 35K08; 42A85; 65T50; 68U10

1. Introduction. Image segmentation is one of the fundamental tasks in image processing. In broad terms, image segmentation is the process of partitioning a digital image into many segments according to a characterization of the image. The motivation behind this is to determine which part of an image is meaningful for analysis. It is one of the fundamental problems in computer vision. Many practical applications require image segmentation, like content-based image retrieval, machine vision, medical imaging, object detection and traffic control systems [14].

The variational method enjoyed tremendous success in image segmentation. In this method, a particular energy is chosen and minimized to give a segmentation of an image. The Mumford-Shah model [15] is the most successful model and has been studied extensively in the last 20 years. More precisely, the Mumford-Shah model was formulated as follows:

$$E_{MS}(u, \Gamma) = \int_{D \setminus \Gamma} |\nabla u|^2 dx + \mu \text{Length}(\Gamma) + \lambda \int_D (u - f)^2 dx \quad (1.1)$$

Here, μ and λ are positive parameters. Γ is a closed subset of D given by the union of a finite number of curves. It represents the set of edges (i.e. boundaries of homogeneous regions) in the image f . The function u is the piecewise smooth approximation to f . Due to the non-convexity of (1.1), the minimization problem is difficult to solve numerically [2].

A useful simplification of (1.1) is to restrict the minimization to functions (i.e. segmentations) that take a finite number of values. The resulting model is commonly

*We thank Prof. Tony Chan, Zuowei Shen, Xuecheng Tai and Xiaoqun Zhang for helpful discussions and suggestions. This research was supported in part by the Hong Kong Research Grants Council (GRF grants 605513 and 16302715, CRF grant C6004-14G, and NSFC-RGC joint research grant N-HKUST620/15).

[†]Department of Mathematics, Hong Kong University of Science and Technology, Clear Water Bay, Kowloon, Hong Kong, China. (dwangaf@connect.ust.hk).

[‡]Department of Mathematics, Hong Kong University of Science and Technology, Clear Water Bay, Kowloon, Hong Kong, China. (hlibb@connect.ust.hk).

[§]Department of Mathematics, Hong Kong University of Science and Technology, Clear Water Bay, Kowloon, Hong Kong, China. (xweiaf@connect.ust.hk).

[¶]Corresponding author. Department of Mathematics, Hong Kong University of Science and Technology, Clear Water Bay, Kowloon, Hong Kong, China. (mawang@ust.hk).

referred to as the piecewise constant Mumford-Shah model. In particular, we have the following two-phase Chan-Vese model [6, 18]:

$$E_{CV}(\Sigma, C_1, C_2) = \lambda Per(\Sigma; D) + \int_{\Sigma} (C_1 - f)^2 dx + \int_{D \setminus \Sigma} (C_2 - f)^2 dx \quad (1.2)$$

where Σ is the interior of a closed curve and $Per(\cdot)$ denotes the perimeter. C_1 and C_2 are averages of f within Σ and $D \setminus \Sigma$ respectively. The level set method was used to solve the minimization problem for the piecewise constant Mumford-Shah functional (1.2). Let $\phi(x) : D \rightarrow R$ be a Lipschitz continuous function with $\Sigma = \{x \in D : \phi(x) > 0\}$ and $D \setminus \Sigma = \{x \in D : \phi(x) < 0\}$. We can rewrite (1.2) as

$$E_{CV}(\phi, C_1, C_2) = \int_D \{\lambda |\nabla H(\phi)| + H(\phi)(C_1 - f)^2 + (1 - H(\phi))(C_2 - f)^2\} dx \quad (1.3)$$

where $H(\cdot) : R \rightarrow R$ is the Heaviside function

$$H(\xi) = \begin{cases} 0 & \text{if } \xi < 0, \\ 1 & \text{if } \xi \geq 0. \end{cases}$$

In practice, a regularized version of H denoted by H_ε is used. Then the Euler-Lagrange equation of (1.3) with respect to ϕ is given by

$$\frac{\partial \phi}{\partial t} = -H'_\varepsilon(\phi) \{ -\{(C_1 - f)^2 - (C_2 - f)^2\} + \lambda \nabla \cdot \left(\frac{\nabla \phi}{|\nabla \phi|} \right) \} \quad (1.4)$$

where

$$C_1 = \frac{\int_D H(\phi) f dx}{\int_D H(\phi) dx} \quad \text{and} \quad C_2 = \frac{\int_D (1 - H(\phi)) f dx}{\int_D (1 - H(\phi)) dx}$$

Equation (1.4) is nonlinear and requires regularization when $|\nabla \phi| = 0$. Various modifications are used in order to solve the equation more efficiently [2, 3, 17, 18].

Esedoglu et al. [11] proposed a phase-field approximation of (1.2) in which the Ginzburg-Landau functional is used to approximate the perimeter:

$$E_{MS}^\varepsilon(u, C_1, C_2) = \int_D \left\{ \lambda \left(\varepsilon |\nabla u|^2 + \frac{1}{\varepsilon} W(u) \right) + u^2 (C_1 - f)^2 + (1 - u)^2 (C_2 - f)^2 \right\} dx \quad (1.5)$$

where $\varepsilon > 0$ is the approximate interface thickness and $W(\cdot)$ is a double-well potential. Variation of (1.5) with respect to u yields the following gradient descent equation:

$$u_t = \lambda \left(2\varepsilon \Delta u - \frac{1}{\varepsilon} W'(u) \right) - 2\{u(C_1 - f)^2 + (u - 1)(C_2 - f)^2\}$$

which can be solved efficiently by an MBO based threshold dynamic method that works by alternating the solution of a linear (but non-constant coefficient) diffusion equation with thresholding.

In a series of papers [7, 8, 9, 16], a frame-based model was introduced in which the perimeter term was approximated via framelets. The method was used to capture key features of biological structures. The model can also be fast implemented using split Bregman method [12].

In [4], a two-stage segmentation method is proposed. In the first stage, the authors apply the split Bregman method[12] to find the minimizer of a convex variant of the Mumford-Shah functional. In the second stage, a K-means clustering algorithm is used to choose $k - 1$ thresholds automatically to segment the image into k segments. One of the advantages of this method is that there is no need to specify the number of segments before finding the minimizer. Any k -phase segmentation can be obtained by choosing $k - 1$ thresholds after the minimizer is found.

Chan et al. [5] considered a convex reformulation to part of the Chan-Vese model. Given fixed values of C_1 and C_2 , a global minimizer can be found. It is then demonstrated in [21] that this convex variant can be regarded as a continuous min-cut (primal) problem, and a corresponding continuous max-flow problem can be formulated as its dual. Efficient algorithms are developed by taking advantage of the strong duality between the primal and the dual problem, using the augmented Lagrangian method or the primal-dual method (see [19, 21] and references therein).

The idea of approximating the perimeter of a set by a non-local energy (using heat kernel) [1][13] is used by Esedoglu and Otto [10] to design an efficient threshold dynamics method for multi-phase problems with arbitrary surface tensions. The method is also generalized to wetting on rough surfaces in [20]. In this paper, we propose an efficient iterative thresholding method for minimizing the piecewise constant Mumford-Shah functional based on the similar approach. The perimeter term in (1.2) is approximated by a non-local multi-phase energy constructed based on convolution of the heat kernel with the characteristic functions of regions. An iterative algorithm is then derived to minimize the approximate energy. The procedure works by alternating the convolution step with the thresholding step. The convolution can be implemented efficiently on a uniform mesh using the fast Fourier transform (FFT) with the optimal complexity of $O(N \log N)$ per iteration. We also show that the algorithm is convergent and has the total energy decaying property.

The rest of the paper proceeds as follows. In Section 2, we first give the approximate piecewise constant Mumford-Shah functional. We then derive the iterative thresholding scheme based on the linearization of the approximate functional. The monotone decrease of the iteration and therefore the convergence of the method is proved (with details given in the appendix). In Section 3, we present some numerical examples to show the efficiency of the method.

2. An efficient iterative thresholding method for image segmentation.

In this section, we introduce an iterative thresholding method for image segmentation based on the Chan-Vese model [6]. The perimeter terms in (1.2) will be approximated by a non-local multi-phase energy constructed based on convolution of the heat kernel with the characteristic functions of regions. The iterative algorithm is then derived as an optimization procedure for the approximate energy. We will also analyse the convergence of the iterative thresholding method.

2.1. The approximate Chan-Vese functional. Let Ω denote the domain of an input image f given by a d -dimensional vector. Our task is to find an n -phase partition $\{\Omega_i\}_{i=1}^n$ of Ω which minimizes (1.2) where Ω_i represents the region of the i^{th} phase. Let $u = (u_1(x), \dots, u_n(x))$ where $\{u_i(x)\}_{i=1}^n$ are the characteristic functions of the regions $\{\Omega_i\}_{i=1}^n$. We then look for u such that

$$u = \operatorname{argmin}_{u \in \mathcal{S}} \sum_{i=1}^n \left[\int_{\Omega} u_i(x) g_i(x) d\Omega + \lambda |\partial\Omega_i| \right], \quad (2.1)$$

where $\mathcal{S} = \left\{ u = (u_1, \dots, u_n) \in BV(\Omega) : u_i(x) = 0, 1, \text{ and } \sum_{i=1}^n u_i = 1 \right\}$; $|\partial\Omega_i|$ is the length of a boundary curve of the region Ω_i ; $g_i = \|C_i - f\|_2^2$ ($\|\cdot\|_2$ denotes the l^2 vector norm) and

$$C_i = \frac{\int_{\Omega} u_i f d\Omega}{\int_{\Omega} u_i d\Omega}. \quad (2.2)$$

It is shown in [1][13], that when $\delta t \ll 1$, the length of $\partial\Omega_i \cap \partial\Omega_j$ can be approximated by

$$|\partial\Omega_i \cap \partial\Omega_j| \approx \sqrt{\frac{\pi}{\delta t}} \int_{\Omega} u_i G_{\delta t} * u_j d\Omega, \quad (2.3)$$

where $*$ represents convolution and

$$G_{\delta t}(x) = \frac{1}{4\pi\delta t} \exp\left(-\frac{|x|^2}{4\delta t}\right)$$

is the heat kernel. Therefore,

$$|\partial\Omega_i| \approx \sum_{j=1, j \neq i}^n \sqrt{\frac{\pi}{\delta t}} \int_{\Omega} u_i G_{\delta t} * u_j d\Omega. \quad (2.4)$$

Hence the total energy can be approximated by

$$\mathcal{E}^{\delta t}(u_1, \dots, u_n) = \sum_{i=1}^n \int_{\Omega} \left(u_i g_i + \lambda \sum_{j=1, j \neq i}^n \frac{\sqrt{\pi}}{\sqrt{\delta t}} u_i G_{\delta t} * u_j \right) d\Omega. \quad (2.5)$$

Now, (2.1) becomes

$$u = \underset{(u_1, \dots, u_n) \in \mathcal{S}}{\operatorname{argmin}} \mathcal{E}^{\delta t}(u_1, \dots, u_n) \quad (2.6)$$

This is a non-convex minimization problem since \mathcal{S} is not a convex set. However, we can relax this non-convex problem to a convex problem by finding $u = (u_1, \dots, u_n)$ such that

$$u = \underset{(u_1, \dots, u_n) \in \mathcal{K}}{\operatorname{argmin}} \mathcal{E}^{\delta t}(u_1, \dots, u_n). \quad (2.7)$$

where \mathcal{K} is the convex hull of \mathcal{S} :

$$\mathcal{K} = \left\{ u = (u_1, \dots, u_n) \in BV(\Omega) : 0 \leq u_i(x) \leq 1, \text{ and } \sum_{i=1}^n u_i = 1 \right\}. \quad (2.8)$$

REMARK 2.1. *It is easy to see that the relaxed minimization problem (2.7) is convex if $C_i (i = 1, \dots, n)$ are constants.*

The following lemma shows that the relaxed problem (2.7) is equivalent to the original problem (2.6). Therefore we can solve the relaxed problem (2.7) instead.

LEMMA 2.1. *Let \mathcal{L} be any linear functional defined on \mathcal{K} and $u = (u_1, \dots, u_n)$. Then*

$$\underset{u \in \mathcal{S}}{\operatorname{argmin}} (\mathcal{E}^{\delta t}(u) + \mathcal{L}(u)) = \underset{u \in \mathcal{K}}{\operatorname{argmin}} (\mathcal{E}^{\delta t}(u) + \mathcal{L}(u)). \quad (2.9)$$

Proof. See Appendix A. \square

2.2. Derivation of the iterative thresholding method. In the following, we show that the minimization problem (2.6) can be solved by an iterative thresholding method. Suppose that we have the k^{th} iteration $(u_1^k, \dots, u_n^k) \subset \mathcal{S}$. Let $g_i^k = \|C_i^k - f\|_2^2$ with

$$C_i^k = \frac{\int_{\Omega} u_i^k f d\Omega}{\int_{\Omega} u_i^k d\Omega}.$$

Then the energy functional $\mathcal{E}^{\delta t}(u_1, \dots, u_n)$ with $g_i = g_i^k$ given above can be linearized near the point (u_1^k, \dots, u_n^k) by

$$\begin{aligned} \mathcal{E}^{\delta t}(u_1, \dots, u_n) &\approx \mathcal{E}^{\delta t}(u_1^k, \dots, u_n^k) \\ &+ \mathcal{L}(u_1 - u_1^k, \dots, u_n - u_n^k, u_1^k, \dots, u_n^k) + h.o.t \end{aligned} \quad (2.10)$$

where

$$\begin{aligned} \mathcal{L}(u_1, \dots, u_n, u_1^k, \dots, u_n^k) &= \sum_{i=1}^n \int_{\Omega} \left(u_i g_i^k + \sum_{j=1, j \neq i}^n \frac{2\lambda\sqrt{\pi}}{\sqrt{\delta t}} u_i G_{\delta t} * u_j^k \right) d\Omega \\ &= \sum_{i=1}^n \int_{\Omega} u_i \left(g_i^k + \sum_{j=1, j \neq i}^n \frac{2\lambda\sqrt{\pi}}{\sqrt{\delta t}} G_{\delta t} * u_j^k \right) d\Omega. \end{aligned} \quad (2.11)$$

We can now determine the next iteration $(u_1^{k+1}, \dots, u_n^{k+1})$ by minimizing the linearized functional

$$\min_{(u_1, \dots, u_n) \in \mathcal{K}} \mathcal{L}(u_1, \dots, u_n, u_1^k, \dots, u_n^k). \quad (2.12)$$

Denote

$$\phi_i^k := g_i^k + \sum_{j=1, j \neq i}^n \frac{2\lambda\sqrt{\pi}}{\sqrt{\delta t}} G_{\delta t} * u_j^k. \quad (2.13)$$

$$= g_i^k + \frac{2\lambda\sqrt{\pi}}{\sqrt{\delta t}} (1 - G_{\delta t} * u_i^k). \quad (2.14)$$

We have

$$\mathcal{L}(u_1, \dots, u_n, u_1^k, \dots, u_n^k) = \sum_{i=1}^n \int_{\Omega} u_i \phi_i^k d\Omega. \quad (2.15)$$

The optimization problem (2.12) becomes minimizing a linear functional over a convex set. It can be carried out at each $x \in \Omega$ independently. By comparing the coefficients $\phi_i^k(x)$ (non-negative) of $u_i(x)$ in the integrand of (2.15), it is easy to see that the minimum is attained at

$$u_i^{k+1}(x) = \begin{cases} 1 & \text{if } \phi_i^k(x) = \min_l \phi_l^k(x), \\ 0 & \text{otherwise.} \end{cases} \quad (2.16)$$

The following theorem shows that the total energy $\mathcal{E}^{\delta t}$ decreases in the iteration for any $\delta t > 0$. Therefore, our iteration algorithm always converges to a minimum for any initial partition.

THEOREM 2.2. *Let $(u_1^{k+1}, \dots, u_n^{k+1})$ be the $k + 1^{\text{th}}$ iteration derived above, we have*

$$\mathcal{E}^{\delta t}(u_1^{k+1}, \dots, u_n^{k+1}) \leq \mathcal{E}^{\delta t}(u_1^k, \dots, u_n^k) \quad (2.17)$$

for all $\delta t > 0$.

Proof. See Appendix B. \square

We are then led to the following iterative thresholding algorithm:

Algorithm: I

Step 0. *Given an initial partition $\Omega_1^0, \dots, \Omega_n^0 \subset \Omega$ and the corresponding $u_1^0 = \chi_{\Omega_1^0}, \dots, u_n^0 = \chi_{\Omega_n^0}$. Set a tolerance parameter $\tau > 0$.*

Step 1. *Given k^{th} iteration $(u_1^k, \dots, u_n^k) \subset \mathcal{S}$, we compute g_i^k and the following convolutions for $i = 1, \dots, n$:*

$$\phi_i^k := g_i^k + \frac{2\lambda\sqrt{\pi}}{\sqrt{\delta t}}(1 - G_{\delta t} * u_i^k) \quad (2.18)$$

Step 2. *Thresholding: Let*

$$\Omega_i^{k+1} = \left\{ x : \phi_i^k(x) < \min_{j \neq i} \phi_j^k(x) \right\} \quad (2.19)$$

and define $u_i^{k+1} = \chi_{\Omega_i^{k+1}}$ where $\chi_{\Omega_i^{k+1}}$ represents the characteristic function of region Ω_i^{k+1}

Step 3. *Let the normalized L^2 difference between successive iterations be*

$$e^{k+1} = \frac{1}{|\Omega|} \int_{\Omega} \sum_{i=1}^n |u_i^{k+1} - u_i^k|^2 d\Omega.$$

If $e^{k+1} \leq \tau$, stop. Otherwise, go back to step 1.

REMARK 2.2. *The convolutions in Step 1 are computed efficiently using FFT with a computational complexity of $O(N \log(N))$, where N is the total number of pixels. Therefore the total computational cost at each iteration is also $O(N \log(N))$.*

REMARK 2.3. *In Step 3, e^k measures the percentage of pixels on which $u_i^{k+1} \neq u_i^k$. Therefore the tolerance τ specifies the threshold of the percentage of pixels changing during the iteration below which the iteration stops.*

3. Numerical Results. We now present numerical examples to illustrate the performance of our algorithm. We implement the algorithm in MATLAB. All the computations are carried out on a MacBook Pro laptop with a 3.0GHz Intel(R) Core(TM) i7 processor and 8GB of RAM.

3.1. Example 1: Cameraman. We first test our algorithm on the standard cameraman image using two-phase segmentation. Figure 3.1(a) is the original image. We start with the initial contour given in Fig. 3.1(b). We choose $\delta t = 0.03$ and $\lambda = 0.01$. Our algorithm takes only 15 iterations to converge to a complete steady state, i.e. $e^k = 0$ (for $k = 15$) with a total computation time of only 0.1188 seconds. Fig. 3.1(c) gives the final segmentation contour. We also plot the normalized energy

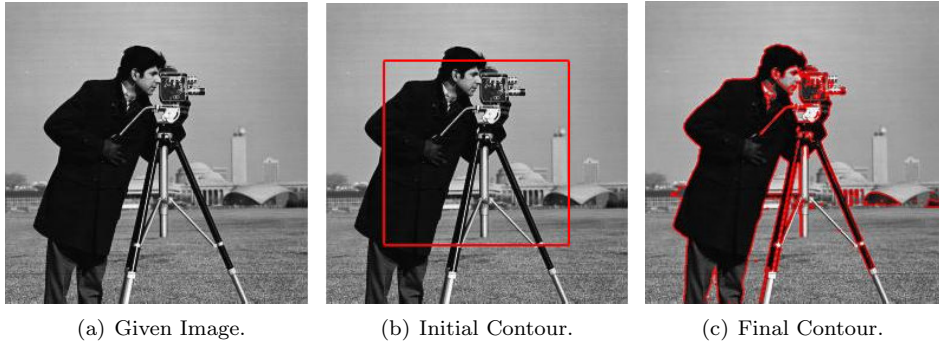


Fig. 3.1: Segmentation results for the classic cameraman image with $\delta t = 0.03$ and $\lambda = 0.01$. The algorithm converges in 15 iterations with a computational time of 0.1188 seconds

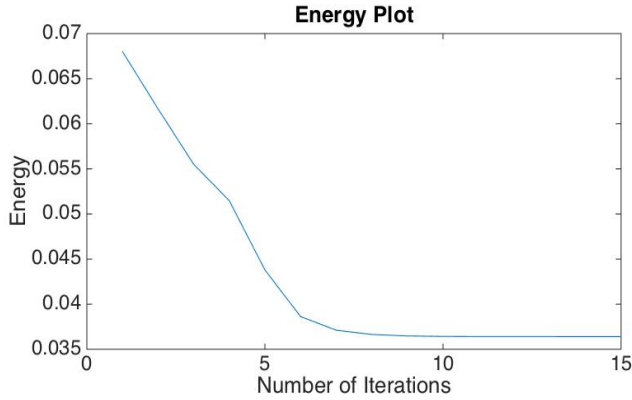


Fig. 3.2: Energy curve for the iteration algorithm with $\delta t = 0.03$ and $\lambda = 0.01$.

$\mathcal{E}^{\delta t}/|\Omega|$ as a function of the iteration number k in Fig.3.2, which verifies the monotone decay of the energy. In fact, the energy decays quickly in the first few iterations and almost reaches steady state in less than 10 iterations.

To study the effect of the parameter λ in the energy (2.5), we run our algorithm on the same test image for three different values of $\lambda = 0.001, 0.01$ and 0.025 but with a fixed $\delta t = 0.03$. The final segmentation contours together with the energy curves are shown in Fig. 3.3. As the figure shows, larger $\lambda = 0.025$ turns to smooth out the small-scale structures while smaller $\lambda = 0.001$ would pick up more noisy regions. This is easy to understand since λ measures the relative importance of the contour length and the data term in the Chan-Vese functional to be minimized. A larger λ tends to shorten the total contour length and therefore does not favor small-scale structures. On the other hand, convergence is much faster for a smaller λ while a larger λ would require more iterations to converge as shown by the energy curves.

3.2. Example 2: A synthetic four-phase image. We next use a synthetic color image given in Fig. 3.4(a). The image f is a vector-valued function. Gaussian

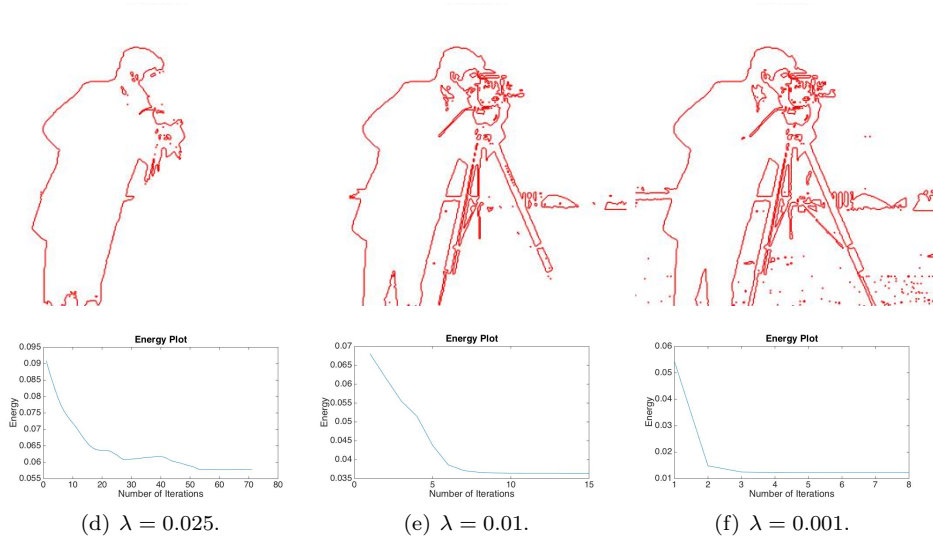


Fig. 3.3: Segmentation contours and energy curves for $\delta t = 0.03$ and different λ values.

noise is added with mean 0 and variance 0.04 to each component of image f . The initial contours are given in Fig. 3.4(b). We apply our four-phase algorithm to the image with three different resolutions from 128×128 to 512×512 . In each case, $\delta t = 0.01$ and $\lambda = 0.003$. The algorithm converges in $7 \sim 8$ iterations for all resolutions with runtimes of 0.0444, 0.1333, 0.6706 seconds respectively, which demonstrates good stability of and robustness of our method. Figures. 3.4(c)-3.4(e) show the final segmentation result.

3.3. Example 3: Flower color image. We now consider an image containing flowers of different colors in Fig. 3.5(a). We first use a two-phase segmentation algorithm with $\delta t = 0.01$ and $\lambda = 0.005$ and the initial contour in Fig. 3.5(b). The algorithm converges in 20 iterations with a runtime of 0.6751 seconds. The final segmentation result is given in Fig. 3.5(c). We also use a four-phase segmentation algorithm with $\delta t = 0.01$ and $\lambda = 0.003$ and the initial contour in Fig. 3.6(a). The algorithm converges in 18 iterations with a runtime of 1.1007 seconds. The final segmentation result is given in Fig. 3.6(b) and 3.6(c)

4. Conclusions. We have proposed an efficient iterative thresholding algorithm for the Chan-Vese model for multi-phase image segmentation. The algorithm works by alternating the convolution step with the thresholding step and has the optimal computational complexity of $O(N \log N)$ per iteration. We prove that the iterative algorithm has the property of total energy decay. The numerical results show that the method is stable and the number of iterations before convergence is independent of the spacial resolution (for a given image). The relative importance of the different effects in the energy functional is studied by tuning the parameter λ . Our numerical results also show that the proposed method is competitive (in terms of efficiency) with many existing methods for image segmentation.

Appendix A. Proof of Lemma 2.1.

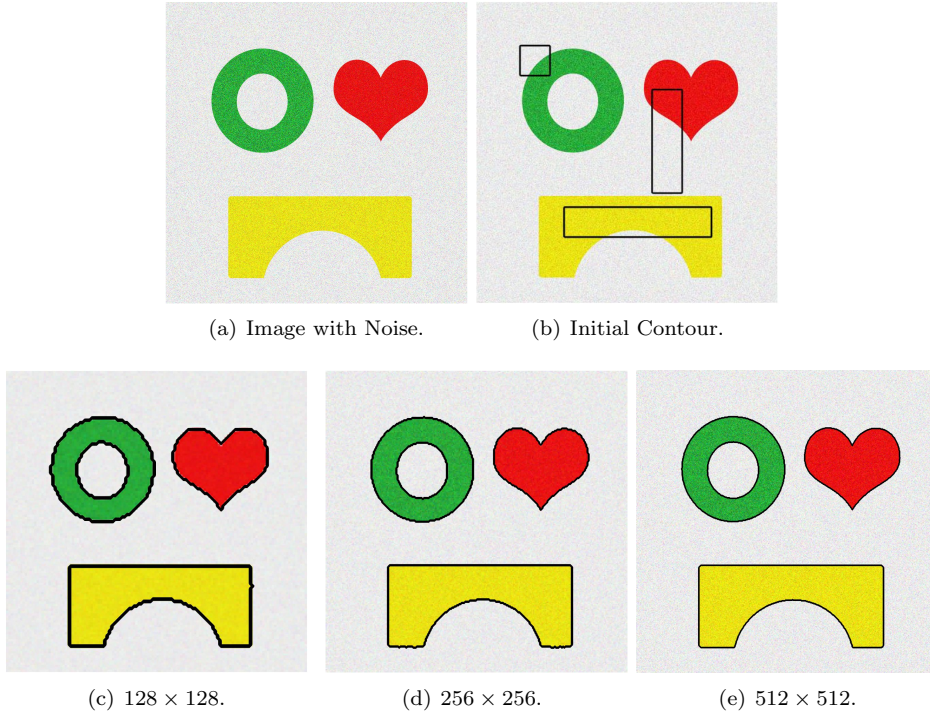


Fig. 3.4: Segmentation for images with different resolutions and with the parameters $\delta t = 0.01$ and $\lambda = 0.003$

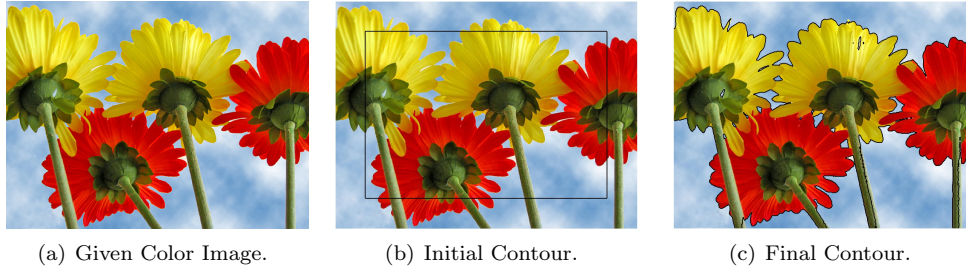


Fig. 3.5: Two-phase segmentation for a 375×500 RGB image and with parameters $\delta t = 0.01$ and $\lambda = 0.005$.

We prove the lemma for the general case that $n \geq 2$ and $d \geq 1$ (i.e. f is a d -dimensional vector valued function) by contradiction. Let $v = (v_1, \dots, v_n) \in \mathcal{K}$ be a minimizer of $\mathcal{E}^{\delta t}(u) + \mathcal{L}(u)$ on \mathcal{K} . If $v \notin \mathcal{S}$, then there exists a set $A \subseteq \Omega$ ($|A| > 0$) and a constant $0 < \epsilon < \frac{1}{2}$ such that for some $k, l \in \{1, \dots, n\}$ with $k \neq l$,

$$v_k(x), v_l(x) \in (\epsilon, 1 - \epsilon), \quad \forall x \in A.$$



Fig. 3.6: Four phase segmentation for a 375×500 RGB image with $\delta t = 0.01$ and $\lambda = 0.003$.

Denote

$$u_m^t(x, t) = v_m(x) + t(\delta_{m,l} - \delta_{m,k})\chi_A(x)$$

for $m = 1, \dots, n$ where $\chi_A(x)$ represents the characteristic function of region A and

$$\delta_{m,l} = \begin{cases} 1 & m = l \\ 0 & m \neq l. \end{cases}$$

When $-\epsilon \leq t \leq \epsilon$, we have $u_m^t(x, t) \geq 0$ and $\sum_{m=1}^n u_m^t(x, t) = 1$ so that $u^t(x, t) = (u_1^t(x, t), \dots, u_n^t(x, t)) \in \mathcal{K}$. Now denote

$$f^m = \int_{\Omega} v_m f d\Omega, \quad V^m = \int_{\Omega} v_m d\Omega, \quad f^A = \int_{\Omega} \chi_A f d\Omega. \quad (\text{A.1})$$

Then

$$\begin{aligned} \int_{\Omega} u_m^t f d\Omega &= \int_{\Omega} v_m f d\Omega + t \int_{\Omega} (\delta_{ml} - \delta_{mk}) \chi_A f d\Omega \\ &= f^m + t(\delta_{ml} - \delta_{mk}) f^A \end{aligned} \quad (\text{A.2})$$

$$\begin{aligned} \int_{\Omega} u_m^t d\Omega &= \int_{\Omega} v_m d\Omega + t \int_{\Omega} (\delta_{ml} - \delta_{mk}) \chi_A d\Omega \\ &= V^m + t(\delta_{ml} - \delta_{mk}) |A| \end{aligned} \quad (\text{A.3})$$

Let

$$C_m = \frac{\int_{\Omega} u_m^t f d\Omega}{\int_{\Omega} u_m^t d\Omega}.$$

It is easy to see that C_m depends on t only when $m = l$ or k . We have

$$C_l = \frac{f^l + t f^A}{V^l + t|A|} \quad \text{and} \quad C_k = \frac{f^k - t f^A}{V^k - t|A|}.$$

Then, we calculate the first and second order derivatives of C_l and C_k with respect

to t as follows:

$$\begin{aligned}
\frac{dC_l}{dt} &= \frac{f^A}{V^l + t|A|} - \frac{|A|(f^l + tf^A)}{(V^l + t|A|)^2} \\
\frac{dC_k}{dt} &= -\frac{f^A}{V^k - t|A|} + \frac{|A|(f^k - tf^A)}{(V^k - t|A|)^2} \\
\frac{d^2C_l}{dt^2} &= -\frac{2|A|f^A}{(V^l + t|A|)^2} + \frac{2|A|^2(f^l + tf^A)}{(V^l + t|A|)^3} \\
\frac{d^2C_k}{dt^2} &= -\frac{2|A|f^A}{(V^k - t|A|)^2} + \frac{2|A|^2(f^k - tf^A)}{(V^k - t|A|)^3}
\end{aligned} \tag{A.4}$$

A direct calculation then gives

$$\begin{aligned}
\frac{d^2\mathcal{E}^{\delta t}}{dt^2} &= \int_{\Omega} \sum_{i=1}^n \left(4 \frac{du_i^t}{dt} \langle C_i - f, \frac{dC_i}{dt} \rangle + 2u_i^t \langle C_i - f, \frac{d^2C_i}{dt^2} \rangle + 2u_i^t \left\| \frac{dC_i}{dt} \right\|_2^2 \right) d\Omega \\
&\quad - 4 \frac{\lambda\sqrt{\pi}}{\sqrt{\delta t}} \int_{\Omega} \chi_A G_{\delta t} * \chi_A d\Omega \\
&= 4 \int_{\Omega} \chi_A \langle C_l - f, \frac{dC_l}{dt} \rangle d\Omega - 4 \int_{\Omega} \chi_A \langle C_k - f, \frac{dC_k}{dt} \rangle d\Omega \\
&\quad + 2 \int_{\Omega} u_l^t \langle C_l - f, \frac{d^2C_l}{dt^2} \rangle d\Omega + 2 \int_{\Omega} u_k^t \langle C_k - f, \frac{d^2C_k}{dt^2} \rangle d\Omega \\
&\quad + 2 \int_{\Omega} u_l^t \left\| \frac{dC_l}{dt} \right\|_2^2 d\Omega + 2 \int_{\Omega} u_k^t \left\| \frac{dC_k}{dt} \right\|_2^2 d\Omega \\
&\quad - 4 \frac{\lambda\sqrt{\pi}}{\sqrt{\delta t}} \int_{\Omega} \chi_A G_{\delta t} * \chi_A d\Omega
\end{aligned} \tag{A.5}$$

where $\langle \alpha, \beta \rangle = \sum_{i=1}^n \alpha_i \beta_i$ for $\alpha, \beta \in R^n$. Evaluating at $t = 0$ and substituting (A.4) into (A.5), we have

$$\left. \frac{d^2\mathcal{E}^{\delta t}}{dt^2} \right|_{t=0} = \int_{\Omega} 4\chi_A \left\langle \frac{f^l}{V^l} - f, \frac{f^A}{V^l} - \frac{|A|f^l}{(V^l)^2} \right\rangle + 4\chi_A \left\langle \frac{f^k}{V^k} - f, \frac{f^A}{V^k} - \frac{|A|f^k}{(V^k)^2} \right\rangle d\Omega \tag{A.6}$$

$$+ 2 \int_{\Omega} v_l \left\langle \frac{f^l}{V^l} - f, -\frac{2|A|f^A}{(V^l)^2} + \frac{2|A|^2f^l}{(V^l)^3} \right\rangle d\Omega \tag{A.7}$$

$$+ 2 \int_{\Omega} v_k \left\langle \frac{f^k}{V^k} - f, -\frac{2|A|f^A}{(V^k)^2} + \frac{2|A|^2f^k}{(V^k)^3} \right\rangle d\Omega \tag{A.8}$$

$$+ 2 \int_{\Omega} v_l \left\| \frac{f^A}{V^l} - \frac{|A|f^l}{(V^l)^2} \right\|_2^2 d\Omega \tag{A.9}$$

$$+ 2 \int_{\Omega} v_k \left\| \frac{f^A}{V^k} - \frac{|A|f^k}{(V^k)^2} \right\|_2^2 d\Omega \tag{A.10}$$

$$- 4 \frac{\lambda\sqrt{\pi}}{\sqrt{\delta t}} \int_{\Omega} \chi_A G_{\delta t} * \chi_A d\Omega. \tag{A.11}$$

Then, using (A.1) and the definition of $|A|$, we can calculate the above integrals (note

that f^l, f^k, f^A, V^l, V^k and $|A|$ in the integrand are all independent of Ω). Therefore,

$$(A.6) + (A.9) + (A.10) \\ = -\frac{2}{V^l} \left\| \frac{|A|f^l}{V^l} - f^A \right\|_2^2 - \frac{2}{V^k} \left\| \frac{|A|f^k}{V^k} - f^A \right\|_2^2 < 0. \quad (A.12)$$

Similarly, direct calculations show that (A.7) = 0 and (A.8) = 0. It is obvious that

$$-4 \frac{\lambda\sqrt{\pi}}{\sqrt{\delta t}} \int_{\Omega} \chi_A G_{\delta t} * \chi_A d\Omega < 0.$$

Combining the above, we have

$$\left. \frac{d^2 \mathcal{E}^{\delta t}}{dt^2} \right|_{t=0} < 0.$$

Thus, $v(x) = u(x, 0)$ cannot be a minimizer. This contradicts the assumption.

Appendix B. Proof of Theorem 2.2. From (2.11), we have

$$\begin{aligned} & \mathcal{E}^{\delta t}(u_1^k, \dots, u_n^k) + \sum_{i=1}^n \int_{\Omega} \sum_{j \neq i, j=1}^n \frac{\lambda\sqrt{\pi}}{\sqrt{\delta t}} u_i^k G_{\delta t} * u_j^k d\Omega = \mathcal{L}(u_1^k, \dots, u_n^k, u_1^k, \dots, u_n^k) \\ & \geq \mathcal{L}(u_1^{k+1}, \dots, u_n^{k+1}, u_1^k, \dots, u_n^k) = \mathcal{E}^{\delta t}(u_1^{k+1}, \dots, u_n^{k+1}) \\ & + \sum_{i=1}^n \int_{\Omega} \left(u_i^{k+1} (g_i^k - g_i^{k+1}) + \sum_{j=1, j \neq i}^n \frac{2\lambda\sqrt{\pi}}{\sqrt{\delta t}} u_i^{k+1} G_{\delta t} * u_j^k \right) d\Omega \\ & - \sum_{i=1}^n \int_{\Omega} \sum_{j \neq i, j=1}^n \frac{\lambda\sqrt{\pi}}{\sqrt{\delta t}} u_i^{k+1} G_{\delta t} * u_j^{k+1} d\Omega. \end{aligned}$$

That leads to

$$\mathcal{E}^{\delta t}(u_1^k, \dots, u_n^k) \geq \mathcal{E}^{\delta t}(u_1^{k+1}, \dots, u_n^{k+1}) + I \quad (B.1)$$

with

$$\begin{aligned} I & = \sum_{i=1}^n \int_{\Omega} \left(u_i^{k+1} (g_i^k - g_i^{k+1}) + \sum_{j=1, j \neq i}^n \frac{2\lambda\sqrt{\pi}}{\sqrt{\delta t}} u_i^{k+1} G_{\delta t} * u_j^k \right) d\Omega \\ & - \sum_{i=1}^n \int_{\Omega} \sum_{j \neq i, j=1}^n \frac{\lambda\sqrt{\pi}}{\sqrt{\delta t}} u_i^{k+1} G_{\delta t} * u_j^{k+1} d\Omega \\ & - \sum_{i=1}^n \int_{\Omega} \sum_{j \neq i, j=1}^n \frac{\lambda\sqrt{\pi}}{\sqrt{\delta t}} u_i^k G_{\delta t} * u_j^k d\Omega \\ & = I_1 + I_2 \end{aligned}$$

where

$$\begin{aligned} I_1 &= \sum_{i=1}^n \int_{\Omega} u_i^{k+1} (g_i^k - g_i^{k+1}) d\Omega \\ I_2 &= \sum_{i=1}^n \sum_{j=1, j \neq i}^n \int_{\Omega} \frac{\lambda \sqrt{\pi}}{\sqrt{\delta t}} u_i^{k+1} G_{\delta t} * (u_j^k - u_j^{k+1}) d\Omega \\ &\quad - \sum_{i=1}^n \sum_{j=1, j \neq i}^n \int_{\Omega} \frac{\lambda \sqrt{\pi}}{\sqrt{\delta t}} (u_i^k - u_i^{k+1}) G_{\delta t} * u_j^k d\Omega. \end{aligned}$$

Now, we only need to prove that $I_1 \geq 0$ and $I_2 \geq 0$. From the definition of C_i^{k+1} and using the fact that $\int_{\Omega} u_i^{k+1} f d\Omega = \int_{\Omega} u_i^{k+1} d\Omega C_i^{k+1}$, we have

$$\begin{aligned} I_1 &= \sum_{i=1}^n \int_{\Omega} u_i^{k+1} (\|C_i^k - f\|_2^2 - \|C_i^{k+1} - f\|_2^2) d\Omega \\ &= \sum_{i=1}^n \int_{\Omega} u_i^{k+1} (\|C_i^k\|_2^2 - \|C_i^{k+1}\|_2^2 - 2\langle C_i^k - C_i^{k+1}, f \rangle) d\Omega \\ &= \sum_{i=1}^n \left\{ \int_{\Omega} u_i^{k+1} d\Omega (\|C_i^k\|_2^2 - \|C_i^{k+1}\|_2^2 - 2\langle C_i^k - C_i^{k+1}, C_i^{k+1} \rangle) \right\} \quad (\text{B.2}) \\ &= \sum_{i=1}^n \left\{ \int_{\Omega} u_i^{k+1} d\Omega \|C_i^k - C_i^{k+1}\|_2^2 \right\} \geq 0. \end{aligned}$$

By changing the order of the two summations in the second part of I_2 and using the fact that $\sum_{i=1}^n u_i^k = 1$ for any k , we obtain

$$\begin{aligned} I_2 &= \sum_{i=1}^n \sum_{j=1, j \neq i}^n \int_{\Omega} \frac{\lambda \sqrt{\pi}}{\sqrt{\delta t}} (u_i^{k+1} - u_i^k) G_{\delta t} * (u_j^k - u_j^{k+1}) d\Omega \\ &= \sum_{i=1}^n \int_{\Omega} \frac{\lambda \sqrt{\pi}}{\sqrt{\delta t}} (u_i^{k+1} - u_i^k) G_{\delta t} * \left(\sum_{j=1, j \neq i}^n (u_j^k - u_j^{k+1}) \right) d\Omega \\ &= \sum_{i=1}^n \int_{\Omega} \frac{\lambda \sqrt{\pi}}{\sqrt{\delta t}} (u_i^{k+1} - u_i^k) G_{\delta t} * (1 - u_i^k - (1 - u_i^{k+1})) d\Omega \quad (\text{B.3}) \\ &= \sum_{i=1}^n \int_{\Omega} \frac{\lambda \sqrt{\pi}}{\sqrt{\delta t}} (u_i^{k+1} - u_i^k) G_{\delta t} * (u_i^{k+1} - u_i^k) d\Omega \geq 0. \end{aligned}$$

Combining (B.1), (B.2) and (B.3) gives (2.17).

REFERENCES

- [1] G. ALBERTI AND G. BELLETTINI, *A non-local anisotropic model for phase transitions: asymptotic behaviour of rescaled energies*, Euro. J. Appl. Math., 9 (1998), pp. 261–284.
- [2] L. AMBROSIO AND V. M. TORTORELLI, *Approximation of functionals depending on jumps by elliptic functionals via Γ -convergence*, Comm. Pure Appl. Math., 43 (1990), pp. 999–1036.
- [3] A. BRAIDES, *Approximation of free-discontinuity problems*, no. 1694, Springer Science & Business Media, 1998.

- [4] X. CAI, R. CHAN, AND T. ZENG, *A two-stage image segmentation method using a convex variant of the mumford-shah model and thresholding*, SIAM J. Imaging Sci., 6 (2013), pp. 368–390.
- [5] T. F. CHAN, S. ESEDOĞLU, AND M. NIKOLOVA, *Algorithms for finding global minimizers of image segmentation and denoising models*, SIAM J. Appl. Math., 66 (2006), pp. 1632–1648.
- [6] T. F. CHAN AND L. A. VESE, *Active contours without edges*, IEEE-IP, 10 (2001), pp. 266–277.
- [7] B. DONG, A. CHIEN, AND Z. SHEN, *Frame based segmentation for medical images*, Commun. Math. Sci., 9 (2010), pp. 551–559.
- [8] B. DONG, H. JI, J. LI, Z. SHEN, AND Y. XU, *Wavelet frame based blind image inpainting*, Appl. Comput. Harmon. Anal., 32 (2012), pp. 268–279.
- [9] B. DONG, J. LI, AND Z. SHEN, *X-ray ct image reconstruction via wavelet frame based regularization and radon domain inpainting*, J. Sci. Comput., 54 (2013), pp. 333–349.
- [10] S. ESEDOĞLU AND F. OTTO, *Threshold dynamics for networks with arbitrary surface tensions*, Comm. Pure Appl. Math., 68 (2015), pp. 808–864.
- [11] S. ESEDOĞLU AND Y.-H. R. TSAI, *Threshold dynamics for the piecewise constant Mumford-Shah functional*, J. Comput. Phys., 211 (2006), pp. 367–384.
- [12] T. GOLDSTEIN AND S. OSHER, *The split bregman method for l_1 -regularized problems*, SIAM J. Imaging Sci., 2 (2009), pp. 323–343.
- [13] M. MIRANDA, D. PALLARA, F. PARONETTO, AND M. PREUNKERT, *Short-time heat flow and functions of bounded variation in r^n* , in Ann. Fac. Sci.Toulouse Math., vol. 16, Université Paul Sabatier, 2007, p. 125.
- [14] A. MITICHE AND I. B. AYED, *Variational and level set methods in image segmentation*, vol. 5, Springer Science & Business Media, 2010.
- [15] D. MUMFORD AND J. SHAH, *Optimal approximations by piecewise smooth functions and associated variational problems*, Comm. Pure Appl. Math., 42 (1989), pp. 577–685.
- [16] Z. SHEN, K.-C. TOH, AND S. YUN, *An accelerated proximal gradient algorithm for frame-based image restoration via the balanced approach*, SIAM J. Imaging Sci., 4 (2011), pp. 573–596.
- [17] A. TSAI, A. YEZZI, AND A. S. WILLSKY, *Curve evolution implementation of the mumford-shah functional for image segmentation, denoising, interpolation, and magnification*, IEEE-IP, 10 (2001), pp. 1169–1186.
- [18] L. A. VESE AND T. F. CHAN, *A multiphase level set framework for image segmentation using the mumford and shah model*, Int’l J. Computer vision, 50 (2002), pp. 271–293.
- [19] K. WEI, X.-C. TAI, T. F. CHAN, AND S. LEUNG, *Primal-dual method for continuous max-flow approaches*, in Computational Vision and Medical Image Processing V: Proceedings of the 5th Ecomas Thematic Conference on Computational Vision and Medical Image Processing (VipIMAGE 2015, Tenerife, Spain, October 19-21, 2015), CRC Press, 2015, p. 17. 00000.
- [20] X. XU, D. WANG, AND X.-P. WANG, *An efficient threshold dynamics method for wetting on rough surfaces*, arXiv:1602.04688, Feb. (2016).
- [21] J. YUAN, E. BAE, AND X.-C. TAI, *A study on continuous max-flow and min-cut approaches*, in Computer Vision and Pattern Recognition (CVPR), 2010 IEEE Conference on, IEEE, 2010, pp. 2217–2224. 00148.